Since January 2020 Elsevier has created a COVID-19 resource centre with free information in English and Mandarin on the novel coronavirus COVID-19. The COVID-19 resource centre is hosted on Elsevier Connect, the company's public news and information website.

Urban Climate 8 (2014) 57–77

Contents lists available at ScienceDirect

Urban Climate

journal homepage: www.elsevier.com/locate/uclim

Practical application of CFD on environmentally sensitive architectural design at high density cities: A case study in Hong Kong

Chao Yuan *, Edward Ng

School of Architecture, The Chinese University of Hong Kong, Shatin NT, Hong Kong

ARTICLE INFO

Article history:
Received 11 June 2013
Received in revised form 26 November 2013
Accepted 3 December 2013

Keywords:
Environmentally sensitivity architectural design
Practical CFD simulation framework
Natural ventilation performance evaluation
Hypothesis testing method

ABSTRACT

Concerns on negative effects of urbanization on the environment make the aerodynamic properties of urban areas increasingly important in architectural design, particularly at high density cities. Over the past few decades, a rapid development in Computational Fluid Dynamics (CFD) has resulted in the widespread use of this technique not only as an environmental research tool but also as an architectural design tool. However, given real building morphologies and particular architectural requirements for the modeling and data analysis, the frequently used methods in research work are unsuitable for practical application. Therefore, this study focuses on the practical application of CFD to bridge the gap between wind engineering and architectural design. This study aims to provide a framework to accurately predict the pedestrian level wind environment, and identify the wind-related design issues. The methods are provided to ans.wer the questions encountered by wind consultants and architects, particularly those on the input boundary condition, simulation modeling, modeling verification, data collection and analysis. The hypothesis testing method is introduced in the framework to verify and evaluate the simulation results. A Hong Kong case study is presented to illustrate that the framework and methods can work well.

1. Introduction

The aerodynamic properties of urban areas are important for pedestrian comfort, wind force on structures, and air pollutant diffusion. Over the last five decades, airflow patterns in urban areas at

* Corresponding author. Tel.: +852 67017286.
E-mail address: yach@cuhk.edu.hk (C. Yuan).

2212-0955/$ - see front matter © 2013 Elsevier Ltd. All rights reserved.
http://dx.doi.org/10.1016/j.uclim.2013.12.001

different scales have been widely studied by wind engineers and meteorologists. Concerns on the negative effects of urbanization on the environment recently make the topic increasingly important for urban planners and architects (Ng, 2009; Bottema, 1995). Tall and compact building blocks seriously worsens the natural ventilation performance at the metropolitan areas, even though there is a large wind potential in the urban atmosphere boundary layer, such as Hong Kong which is a high-density coastal city. The natural ventilation is an important contributing factor to outdoor thermal comfort, especially in subtropical cities. Cheng et al. (2012) indicated that, taking the Physiologically Equivalent Temperature (PET) thermal comfort as a standard, wind speed decreasing from 1.0 to 0.3 m/s is equal to 1.9 °C air temperature increase in the subtropical summer. Good planning and design which include the wind knowledge can mitigate negative effects of urbanization, particularly urban heat island intensity (Oke, 1987). Furthermore, these planning and design make compact urban living environments more comfortable for residents and consequently aid in the restriction of uncontrolled urban spreading (European Environment Agency, 2006; Garreau, 1992).

This study aims to change the traditional experience-based design way toward a scientific wind-environment-sensitive architectural design, and ensures that the surrounding environment of the proposed buildings could be adequately considered. To mitigate the undesirable effects of the proposed buildings on the surrounding natural ventilation performance, four steps for knowledge-based decision making are significantly important in the design process. The first step is the analysis and simplification of local wind availability. Local wind availability is important for initial wind assessment at the urban scale. Furthermore, local wind data is necessary for the settings of the boundary condition for wind environment modeling at the city and building scales. The second step involves the modeling of the surrounding pedestrian airflow. The modeling results make detailed wind data available to all of wind engineers, urban planners, and architects for better understandings. The third step is the wind data collection. Both unbiased descriptions of the surrounding wind environment and critical wind-related design issue identification depend on an appropriate data collection process. Based on the robust application of the above three steps, the fourth step, the data interpretation can be confidently conducted. This step is critical in the decision-making process for building design implementation. A sufficient statistical analysis is necessary to summarize the collected wind data and correlate the modeling results with architectural design strategies. Then, knowledge-based decisions can be made by architects and urban planners.

However, the methods used to follow the aforementioned steps in the research work, such as simplification of the input wind availability, analysis of the grid dependence, the influence of iterative convergence, data collection and analysis methods, are unsuitable for the real application because of the characteristics of the practical CFD application in the architectural design process. Compared with the modeling in the research work, the input conditions and proposed building morphologies are much more complicated in the real application. Requirements of architects in the data analysis are also very different with wind engineers and researchers. Thus, the current study focuses on the practical application of CFD simulation and aims to answer the questions that are often encountered by practicing wind consultants, architects, and planners: (1) how to set the appropriate boundary conditions, (2) how to verify the CFD simulation results in practical applications, and (3) how to collect and evaluate the simulation results to efficiently and accurately identify the important wind-related design issue for implementation. A procedural framework and methodologies for the practical application of CFD simulations in real architectural design process are provided in this study to make the CFD simulation more practical and dependable, as well as to make the results more helpful in architectural design. A case study in Hong Kong is conducted to illustrate how the proposed framework and methodologies can be used.

2. Understanding the boundary condition (local wind availability)

The boundary condition is the local wind availability at the surrounding areas of the proposed new projects. Before the advent of modeling, wind data at the urban areas can be collected by using field measurement. However, given the limitations and difficulties in applying field measurement at urban areas (Oke, 2004, 2006), the large scale modeling became a popular approach for the reproduction and

prediction of urban wind environment. Both surface roughness modeling and meso-scale airflow modeling are necessary to analyze the local wind availability, providing information for the setting of boundary conditions. Surface roughness modeling (morphologic method) is used to evaluate the effects of the surrounding urban morphology on the incoming airflow pattern. Meso-scale airflow modeling (physical and numerical modeling) is used to directly reproduce incoming airflow physically or numerically in the Atmospheric Boundary Layer (ABL).

2.1. Surface roughness modeling (Morphologic method)

At the urban scale, buildings can be treated as the surface roughness elements. Although the effect of the pressure drag of each building dominates the turbulent flow in the street canyon, the effects of pressure drag can be normalized or aggregated as the skin friction drag (shear stress) that results from the friction between large urban surfaces and air flow. This knowledge is considered as the quasi-physical reasoning that Prandtl's boundary layer theory presented in 1904 (Anderson, 2005), the logarithmic wind profile, is valid for the airflow structure above the large urban area (Oke, 1987). It is valid from z_{min} to z_{max} (the range of the thin shear layer), $z_{min} \gg z_0$ (surface roughness length), and $z_{max} \ll \delta$ (boundary layer height) (Bottema, 1996).

Bottema (1996) stated that the vertical velocity gradient is the roughness constant in the Roughness Sub Layer (RSL), except several inhomogeneous horizontal flow (Arnfield, 2003). Above z_r (the blending height), at the top of the RSL, turbulence mixing becomes sufficient to "blend" the flow independent of the horizontal position (Garratt, 1978). Notably, the height of z_r depends on the urban density [1.5 z_H (averaged building height) for high-density areas; 4 z_H for low-density areas] (Oke, 2004). From z_r to δ, the inhomogeneous building geometry length scales can be spatially-averaged by z_0 [similar to κ_0 (Kármán constant) in the wall function of CFD], and the wind speed gradient in this layer can be estimated by z_0 and z_d (displacement height) using the logarithmic equation.

The importance of the aforementioned knowledge in wind engineering and urban design lies in the capability of aerodynamic properties to describe the urban surface roughness. Two methods are available for surface roughness modeling: surface roughness classification (Davenport et al., 2000) and morphometric modeling method (Bottema, 1995; Counihan, 1971; Grimmond and Oke, 1999; Kutzbach, 1961; Lettau, 1969; MacDonald et al., 1998; Raupach, 1992). Surface roughness classification is based on the repeatable and verified field observation results. Given its feasibility and accuracy, roughness classification is often used to set the surrounding surface roughness as a boundary condition in practical applications of CFD simulation. However, if the types of surfaces are significantly different at the surrounding areas (resulting in insufficient fetch length for each surface type), selecting a single classification to represent roughness of the entire surrounding area becomes difficult.

The morphometric method for the estimation of surface roughness (z_0 and z_d) is currently popular for its capability to test the spatial difference of the surface roughness in large continuous urban areas. The method makes the setting of the appropriate surrounding surface roughness easier. Grimmond and Oke (1999) conducted a broad and critical review to introduce various morphological models and to compare their sensitivities. Several models are only valid for low-density areas (Counihan, 1971; Kutzbach, 1961; Lettau, 1969; Raupach, 1992): ku_d and ku_0: $\lambda_p \leqslant 0.29$; Le_0: $\lambda_f \leqslant 02\sim0.3$; Co_0: $\lambda_p \leqslant 0.5$; Ra_0: $\lambda_f \leqslant 0.25$. Although recently available models (Bottema, 1996; MacDonald et al., 1998) attempted to extend the limitation for large surface roughness, such as built areas, z_0 meets the peak value with increasing roughness because of the skimming flow (Grimmond and Oke, 1999) (z_0 meets the peak for λ_f, which is approximately 0.2 in Bottema's model (Bottema, 1996). Therefore, z_d always has to be incorporated into the estimates of the surface roughness at urban areas.

2.2. Mesoscale airflow modeling (Physical and numerical method)

Mesoscale airflow modeling is used to model the airflow pattern in the atmospheric boundary layer directly. Therefore, except for the surrounding surface roughness, another important boundary condition, the incoming wind velocity at the reference height, can be estimated by using meso-scale airflow modeling: boundary-layer wind tunnel or numerical modeling.

The use of a non-aeronautical wind tunnel for the atmospheric boundary layer is based on two important theories: (1) Prandtl's theory (logarithmic profile for wind speed); (2) scale model theory: the same ratio of z_H to z_0 in the model and prototype (Plate, 1982). Plate (1999) reviewed several important issues for the wind tunnel experiment, such as the scaled modeling, input wind profile setting, and application framework of wind tunnel in urban planning. Kubota et al. (2008) conducted a 1:300 wind tunnel experiment to test the effect of local building density on pedestrian-level wind velocities. The atmospheric transport and dispersion around the World Trade Center site were examined by a 1:600 scale wind tunnel experiment (Perry et al., 2004). In Hong Kong, the Wind/Wave Tunnel Facility conducted experiments to understand the wind availability and flow characteristics at metropolitan areas (Hong Kong Planning Department, 2008), which were frequently used as the input data for city-scale CFD simulation.

Three-dimensional mesoscale boundary-layer turbulence closure numerical models, which have been rapidly developed since the 1970s' (Mellor and Yamada, 1974, 1982), are mainly applied to solve geophysical fluid problems in the planetary boundary layer (Pielke et al., 1992; Yamada and Bunker, 1989). Regional numerical weather predictions were realized by integrating turbulence closure models with heat exchange and energy balance models to describe and predict atmospheric mesoscale phenomena.

With the increasing concern on urban environmental issues, such as urban morphology, land-use, and anthropogenic heat emission, researchers have attempted to downscale the weather forecast modeling to test urbanization effects on the urban environment, such as urban heat island and air pollutant distribution.

Associated with the surface energy balance model, higher order turbulence model for atmospheric circulation, called the Mellor–Yamada hierarchy model (level 2.5), was used to test the effects of land use on the urban environment (Mochida et al., 1997; Murakami, 2004). The domain of regional-scale simulation covered 480 km × 480 km × 5 km. The uniform horizontal grid size was 8 km × 8 km, and the vertical grid space was enlarged from 4 m above the ground by using a total of 20 vertical layers. The simulation at the local scale can be performed in the high resolution because of the super computational capability of the Earth simulator. Ashie et al. (2009) used the standard κ-ε turbulence model with integration of the buoyancy of vapor and Coriolis force to simulate Tokyo's heat island phenomenon in very high resolution (5 m square horizontal and 1 m –10 m vertical intervals in a 3 km × 3 km × 500 m domain: approximately 5×10^9 grid points). Given the high resolution, the wind velocity data at 5 m above ground was available to evaluate local wind availability. A similar simulation for Hong Kong was conducted in 2011 to verify the research on urban climatic map analysis (Ng, 2012).

The National Center for Atmospheric Research (NCAR) in America successively provided two mesoscale prognostic weather models: the fifth-generation NCAR Mesoscale model (MM5) (Grell et al., 1994) and the Weather Research and Forecasting (WRF) (Skamarock et al., 2005). MM5 was successfully used in large-scale wind environment research (Dudhia, 1993; Berg and Zhong, 2005). Combining the MM5 model with the California Meteorological Model (CALMET) model (Scire et al., 2000), Yim et al. (2007) calculated the local wind availability in Hong Kong in high resolution (resolutions in MM5 and CALMET: 1 km and 100 m). WRF, as the next-generation prognostic weather model, is currently very popular and is increasingly being applied in urban environment research by coupling with the data set of the urban morphology (Chen et al., 2011).

Given that the real airflow is used in the wind tunnel experiment, the wind data reproduced in the wind tunnel experiment is much more accurate than the estimation in the numerical modeling, which is based on several basic assumptions for the turbulence flow. However, the turbulent flow, heat exchange, energy balance, vapor buoyancy, and even the Coriolis force can be coupled in the numerical modeling. This coupled modeling is impossible to the wind tunnel experiment. With the rapid computer capability development, higher resolution and more advanced physical models are being applied in simulations to improve the accuracy.

3. Understanding the airflow modeling process

To model the turbulent flow in the urban canyon, the wind tunnel (physical modeling) and CFD simulation (numerical modeling) are two broadly used approaches. Given the commercial codes

and advanced computational capability, the last decades have seen the remarkable rapid development of CFD simulation in environmental design. CFD simulation has already been used not only as an environmental research tool to broaden predictive power, but also as a design tool for urban planners and designers (Murakami, 2006). In the building/city block scales, CFD was conducted for both real cases (Blocken et al., 2012; Letzel et al., 2008) and research work (Gousseau et al., 2010; Mochida et al., 2002; Salim et al., 2011; Tominaga et al., 2008; Yoshie et al., 2007).

In CFD simulation, users have to make numerous decisions about the computational settings, including the domain size, grid structure, turbulence model options, and convergence criteria. The simulation accuracy significantly depends on these issues. Therefore, the simulation accuracy depends on the user experience and skill. For pedestrian-level wind assessment, the working group from the Architectural Institute of Japan (AIJ) provided a practical guideline based on cross-comparisons between wind tunnel data and simulation results in numerous scenarios with different modeling settings (Tominaga et al., 2008). Compared with the AIJ guideline, a similar guideline (COST 14) was based on the broad relative literature review (Frank, 2006). Blocken et al. (2007) reported a guideline for the wall function to avoid unexpected wind speed acceleration in the stream-wise direction. Apart from the aforementioned guidelines, the validation for CFD simulation by comparing with existing wind tunnel or field measurement data is always required in the research work.

However, several problems make it difficult to ensure the accuracy of real-case simulations. First, apart from the setting issues clearly stated in the current guidelines (Frank, 2006; Tominaga et al., 2008), several important issues, such as grid dependence and convergence criteria, remain unclear. On one hand, because of the sophisticated real building morphologies, the quality of the mesh structure in real cases is not as good as that in parametric study, in which only simplified morphologies are used. Therefore, following the strict requirements for convergence criteria in real cases is more difficult than in parametric studies. COST 14 states that a reduction in scaled residuals of at least four orders of magnitude is required (Frank, 2006). A practical criterion of iterative convergence is needed for real case studies. On the other hand, given that real case conditions are always different, using a unified criterion for the grid dependence is also difficult.

Secondly, unlike validation in parametric studies, validating the CFD simulation result in the practical applications by comparing the results of a generic model with existing wind tunnel data, so called sub-configuration validation (Blocken et al., 2012), is unsuitable. This method is time and resource consuming and is thus impractical for the architectural designing process. Furthermore, although efficient validation results can be obtained from the genetic model, such results still cannot validate the simulation results in real cases. It is because that the mesh structure in the generic model and that in real case studies are totally different. The grid is important for the modeling results (Tominaga et al., 2008). Furthermore, using field measurements to validate CFD simulation for non-existing proposed building design options is impossible.

4. Understanding the data collection and interpretation for application

The data analysis must be scientific to provide the accurate and unbiased understandings for architects. Less noticed, but equally important, data analysis for architects is to interpret the modeling results for the architectural design practice (Ng, 2012). It must be straightforward and relate the phenomenon of surrounding airflow with particular design strategies or indexes. It is significantly different with the data analysis for wind engineers and researchers, in which the wind field is mathematically described by various turbulence flow index profiles.

Most CFD software packages provide the post-process program by which the global wind field can be presented by a wind speed contour or vector. This kind of result visualization is one of the advantages of CFD simulation over wind tunnel experiments. For architects and planners, the result visualization is the intuitive grasp of the target wind environment. However, the global visualization of the wind environment is insufficient for identifying the optimal design option and for quantitatively determining whether the adopted mitigation strategies are sufficient. Furthermore, to analyze the annual or seasonal wind environment, the data analysis in the practical application always needs to include the simulation results in several input wind directions, according to the annual or seasonal

wind probability. Making robust decisions by observing numerous visualized simulation results together becomes difficult.

Therefore, except for the visualized simulation results, the statistic analysis of the wind speed frequency and distribution are required to evaluate the global natural ventilation performance (Yuan and Ng, 2012). On the other hand, the statistical integration of simulation results in different input wind directions is needed. Furthermore, aside from the global evaluation, the analysis method is also needed to evaluate the natural ventilation performance at the particular locations with design strategic importance.

5. Framework and methodology

Based on the discussion in Sections 2–4, a procedural framework for the practical application of CFD simulation in architectural design is presented as shown in Fig. 1. In step 1, the appropriate modeling methods have to be chosen to initialize the boundary condition in the CFD simulation: calculating the surrounding surface roughness and input wind data (wind speeds at the reference height). According to the review in Section 2, the appropriate modeling methods can be chosen based on particular modeling needs, available computer capability, and input data sources.

In step 2, based on the discussion in Section 3, the accuracy of CFD simulation can be verified by using existing practical guidelines and sensitivity tests for grid dependence and iterative convergence criteria. In the sensitivity tests, two testing scenarios were modeled in a similar manner, except that the scenarios have different grid point numbers or convergence criteria. The hypothesis testing (ANOVA) and regression analysis were conducted to determine whether significant differences exist between the match pair. If the wind data distributions in different scenarios are similar (without significant difference), the simulation results are independent of the grid point number or convergence

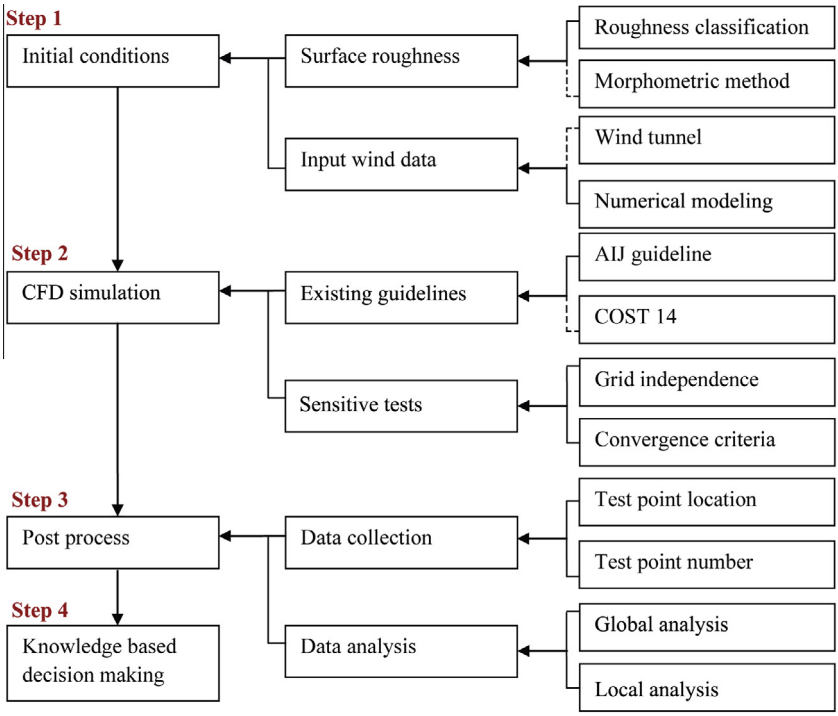

Fig. 1. Framework for the practical application of CFD simulation in the architecture design. The alternatives which are not applied in the following case study are presented as dash lines.

criteria. Among them, the lower standards of the grid point number and convergence criteria can be applied to decrease the computational cost. If the distributions are significantly different, more testing scenarios are needed until the acceptable threshold values for the grid point number and convergence criteria are determined.

Step 3 involves data collection and interpretation for the architectural design process. To ensure that the post-process is sufficient for knowledge-based decision making, scientific decisions should be based on the statistical modeling of the wind data collected at the appropriate test points; that is, the test point location has to be unbiased, and the test point number should be adequate. As shown in Fig. 1, data analysis should be globally and locally conducted to evaluate both the effects of proposed building on the whole surrounding wind environment and the effects on the local areas with design strategy importance. Both of them are significantly important for the decision making in the architectural design process.

First, a description of the pedestrian-level wind environment for all scenarios (different design options in different prevailing wind directions) is presented by using global wind contour and vector maps over the entire modeling area. Thus, architects can quickly grasp the effects of the proposed building on the surrounding wind environment.

Second, statistical modeling is used to integrate the wind conditions in several prevailing wind directions and to prescribe the averaged natural ventilation performance for the further evaluation of the wind environments. Cooperating with the aforementioned wind contour and vector maps, the analysis can facilitate quantitative understanding of the surrounding wind environments, which is especially useful for the cross-comparison of different design options.

In the statistical modeling of this study, the distribution of the overall wind velocity ratio ($VR_{w,j}$) is used. The $VR_{w,j}$ for each test point is calculated as (Hong Kong Planning Department (HKPD), 2008):

$$VR_{w,j} = \sum_{i=1}^{n} P_i \cdot VR_{i,j} \tag{1}$$

where P_i is the annual probability of the prevailing wind approaching the target area from the direction (i), and n is the number of prevailing wind directions considered in the simulation. $VR_{i,j}$ is the wind velocity ratio in the particular wind direction (i). $VR_{i,j}$ can be calculated as (HKPD, 2008):

$$VR_{i,j} = \frac{V_{p,i,j}}{V_i} \tag{2}$$

where $V_{p,i,j}$ is the j-th test point's wind velocity at the pedestrian level in a particular wind direction (i), and V_i is the wind velocity at the reference height in a particular wind direction (i).

Third, the wind data of test points located at areas with strategic importance is statistically analyzed by the wind velocity ratio polar. The wind velocity ratios in different input prevailing wind directions at a test point are plotted into a wind rose. This method can provide more detailed information than global evaluation, such as the reason why the $VR_{w,j}$ of test points are lower than expected, as well as the identification of parts of a building which block airflow in certain input wind directions. This kind of understandings is useful for architects to optimize the optional design options.

6. Case study in Hong Kong

6.1. Background

Hong Kong is a high-density subtropical city that has undergone rapid urbanization since the 1960s. There are 7 million people living within at a 272 km^2 urban area. Given the outbreak of Severe Acute Respiratory Syndrome in 2003, the Hong Kong Planning Department (HKPD) initialized a study on air ventilation assessment (AVA) to improve natural ventilation performance (HKPD, 2005). The AVA followed the ethos of "the more wind, the better". Sustainable Building Design Guidelines (Technical circular No. 1/06) was published (Hong Kong Building Department (HKBD), 2006). However, in the current technical circular, CFD simulation was not recommended: "*CFD may be used with caution... There is no internationally recognized guideline or standard for using CFD in outdoor urban scale studies.*"

Furthermore, this technical circular did not include the guidelines for data analysis for the architectural design process.

Therefore, a case study of Hong Kong is conducted to illustrate how well the procedural framework and methodologies presented in this study can work for the practical CFD simulation. In this case study, the proposed building is long, and the gap between the proposed building and other adjacent existing buildings is limited. Thus, design strategies are needed to mitigate the negative effects of the proposed building on the surrounding wind environment. Three design options with different mitigation strategies are provided by the Architecture Service Department (ASD). CFD simulation by using ANSYS 14 (Adopted for meshing: ICEM; Adopted for CFD simulation: Fluent) is conducted to compare the effects of these three options on the surrounding wind environment and to identify the optimal design option.

As shown in Fig. 2, in design option 1, two air passageways at the ground floor are provided and arranged at the north and south sides of the proposed building. Except for the low-zone passageways, building porosity in the upper floor is also applied in this design option. In design option 2, wider air passageways are provided at the ground floor. More importantly, an air passage ways is arranged at the middle of the proposed building, where building permeability could be more efficient to improve the natural ventilation performance at the leeward areas. The design option 3 is established based on design option 2. Apart from the different details on building morphologies, wider air passageways and larger building porosity than in design option 2 are applied in design option 3.

6.2. Boundary condition settings

The boundary condition consists of input, output wind data, and surface roughness. The annual local wind data on the site are derived from a coupled MM5/CALMET model (Yim et al., 2007) and are simplified as input wind data in the CFD simulation as follows: annually averaged wind speed at the

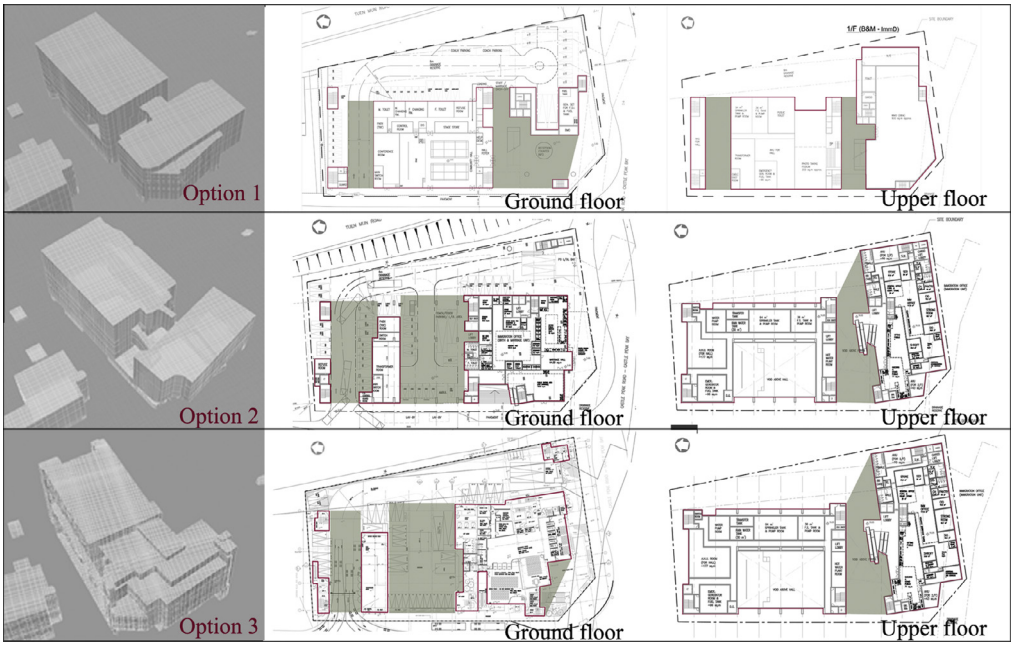

Fig. 2. Description of the three design options and mitigation strategies. The air passageways at the ground and upper floors are identified as green shaded areas.

reference height (120 m) and wind probability in seven prevailing wind directions, which are highlighted in Table 1. The major prevailing wind directions are selected by following the requirement from the Sustainable Building Design Guidelines (technical circular No. 1/06): "*the probability of wind coming from the reduced set of directions should exceed 75% of the time in a typical reference year*" (HKBD, 2006). Surface roughness is set based on the surface roughness classification in the Architectural Institute of Japan (AIJ) guidelines (Tominaga et al., 2008). Therefore, the input vertical wind speed profile can be set as:

$$V_h = V_{met} \cdot \left(\frac{h}{d_{met}}\right)\alpha \tag{3}$$

where α is the surface roughness factor (0.35) (AIJ, 2007) due to the high urban density at Hong Kong, V_{met} (Table 1) is the mean wind speed from an individual wind direction at 120 m, and d_{met} is the reference height 120 m above the ground at which the airflow is unaffected by the urban roughness below (boundary layer height) (Tominaga et al., 2008). The outflow boundary condition is set as a pressure boundary condition with dynamic pressure equal to zero. The logarithmic law boundary is used as the wall boundary.

6.3. Simulation modeling

In this section, CFD simulation is conducted to reproduce the airflow in the three design options. To ensure the accuracy of the simulation, the modeling setting followed the AIJ guidelines and technical circular No. 1/06 (Tominaga et al., 2008; HKBD, 2006). Furthermore, sensitivity tests for grid dependence and convergence criteria are conducted.

6.3.1. Computational domain and models

The computational domains for all design option cases are same: 1200 m × 1200 m × 250 m, as shown in Fig. 3. The blockage ratio (R_b) is calculated as:

$$R_b = \frac{V_{\text{model}}}{V_{\text{domain}}} \tag{4}$$

where V_{domain} is the domain volume 3.6×10^8 m^3, and V_{model} is the model volume which is estimated by the area covered by the topology and buildings as 91,204 m^3. If the average model height is assumed to be 100 m, the blockage ratio will be 2.5%. Considering that the height of all buildings and topologies is less than 100 m, the blockage ratio in this study is less than 3%.

Table 1
Annual wind availability data on site from MM5/CALMET model (The selected prevailing wind directions are highlighted).

Wind directions (i)	Mean wind speed (m/s)	Wind probability (%)
N (0°)	7.1	3.9
NNE (22.5°, i = 1)	**10.6**	**13.1**
NE (45°, i = 2)	**9.5**	**14.3**
ENE (67.5°, i = 3)	**6.1**	**7.8**
E (90°, i = 4)	**5.7**	**5.2**
ESE (112.5°, i = 5)	**7.2**	**11.8**
SE (135°, i = 6)	**6.2**	**13.0**
SSE (157.5°, i = 7)	**6.0**	**9.9**
S (180°)	5.2	5.1
SSW (202.5°)	4.8	4.4
SW (225°)	5.7	3.7
WSW (247.5°)	5.0	2.2
W (270°)	4.8	1.1
WNW (292.5°)	5.2	0.8
NW (315.5°)	6.2	1.5
NNW (337.5°)	6.3	1.5

As shown in Fig. 4, a 400 m × 400 m modeling area is established. This area is sufficient to include the surrounding buildings and topology (>2H, H being the height of the tallest building on site). As shown in Fig. 2, the target buildings (design options 1, 2, and 3) are established based on the Computer-Aided Design (CAD) files provided by ASD.

6.3.2. Grid arrangement

Finer grids are generally arranged at a 400 m × 400 m modeling area, and coarse grids are arranged at less important surrounding areas. Based on the AIJ guidelines, three layers (layer height: 0.5 m) are arranged below the evaluation height (fourth layer, 2 m above the ground), as shown in Fig. 5. The maximum grid size ratio is set to 1.3, as required by the AIJ guidelines.

6.3.3. Sensitivity test for grid dependence

As the framework suggested by Frank et al. (2012), the successively refined resolutions are tested for grid dependency. Three similar simulations, which only differ in grid point number (Grid 1: 7.0 million, Grid 2: 5.5 million, and Grid 3: 3.0 million), are conducted for the grid dependence tests. In this matched-pair group, wind speeds are measured at the 35 test points which are plotted at Fig. 6. The number of test points (n = 35) is determined to comply with the requirements for constructing robust hypothesis tests. More details on the test point locations are introduced in Section 6.4 for data analysis.

Inferential statistics by using t-distribution is conducted to test the sensitivity of the simulation result on the grid resolution. The difference of wind speeds in the three scenarios with different grid resolutions is determined. According to the p-value (>0.05) given in Table 2a, no sufficient evidence is present to conclude that the wind data simulated in the resolutions of Grid 1 and 2 differ at the level of significance (0.05). However, as shown in Table 2b, the p-value (<0.05) in the hypothesis test for

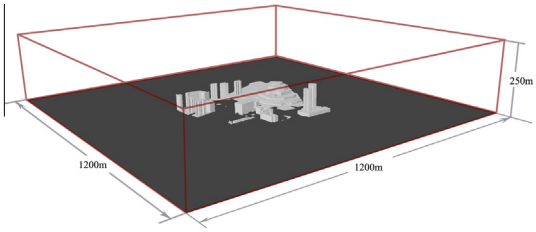

Fig. 3. Computational domain size.

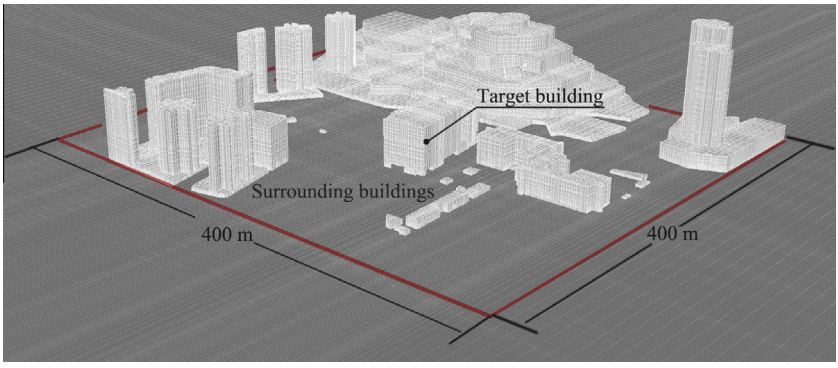

Fig. 4. 400 m × 400 m modeling area. The target is located at the center building.

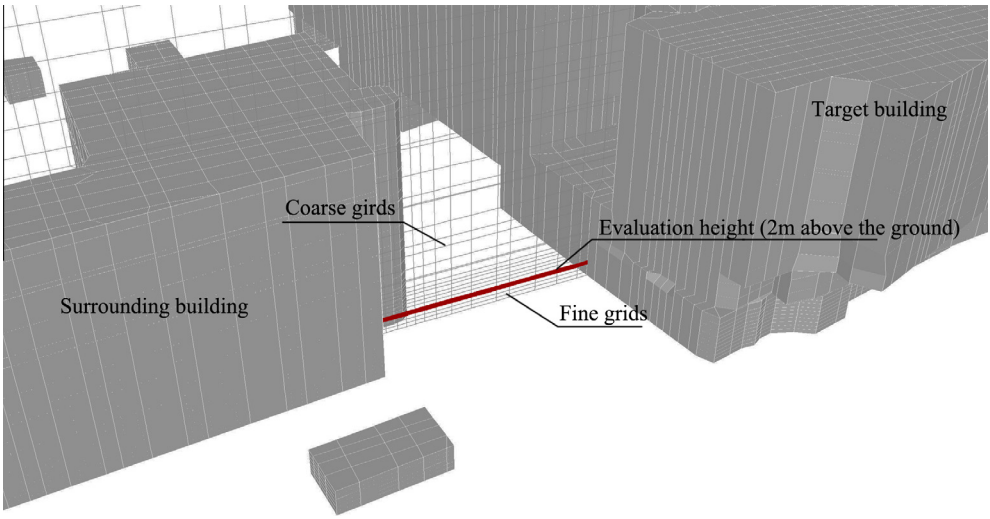

Fig. 5. Modeling area adjacent to the building to clarify the first four layers parallel to the ground surface and the evaluation height.

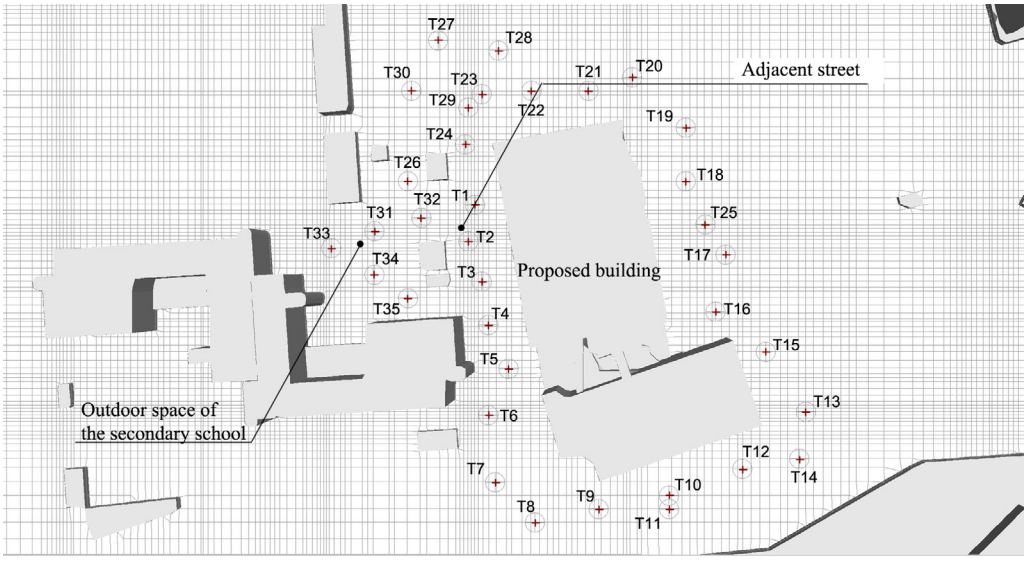

Fig. 6. Test point locations (sample size n = 35). Two areas with strategy importance (outdoor space of the secondary school and adjacent street) are pointed out.

Grid 1 and 3 indicates a significant difference between two simulation results at the level of significance (0.05). That is, both of Grid 1 and 2 are suitable for resolving the turbulence flow in this case study, and the resolution in Grid 3 is not high enough. To decrease the computing cost, the grid resolution in Grid 2 is adopted.

Table 2a
Paired Samples Hypothesis Test (the significant level: 0.05; sample size: $n = 35$).

	Paired differences					t	Sig. (2-tailed) (P-value)
	Mean	Std. deviation	Std. error mean	95% Confidence interval of the difference			
				Lower	Upper		
Grid resolution_1–Grid resolution_2	.00543	.08219	.01389	−.02280	.03366	.391	.698

Table 2b
Paired Samples Hypothesis Test (the significant level: 0.05; sample size: $n = 35$).

	Paired differences					t	Sig. (2-tailed) (P-value)
	Mean	Std. deviation	Std. error mean	95% Confidence interval of the difference			
				Lower	Upper		
Grid resolution_1–Grid resolution_3	.06508	.20725	.03503	−.00612	.13627	1.858	.072

Table 3
Different scaled residuals in the simulations.

	Continuity	U-x (m/s)	U-y (m/s)	U-z (m/s)	Energy (J)	K (m^2/s^2)	Omega (1/s)
Criterion_1	4.26E-05	1.13E-06	1.08E-06	6.07E-07	5.10E-08	1.35E-05	1.97E-06
Criterion_2	2.70E-04	7.77E-06	7.56E-06	4.49E-06	5.64E-08	7.72E-04	1.71E-05
Criterion_3	1.01E-03	7.76E-05	8.16E-05	5.26E-05	5.82E-08	1.27E-03	9.04E-05

6.3.4. Turbulence model

The turbulence model provided by ANSYS Fluent 14.0 is used in this study. The κ-ω SST (Shear Stress Transport) model is chosen, which comprises the standard κ-ω model as the near-wall model and the κ-ε model as the model for the outer part of the near-wall region (Menter et al., 2003; Fluent Inc., 2012). The accuracy of the SST κ-ω model is validated by comparing the simulation results with the existing wind tunnel data (2:1:1 shape building model) from AIJ (Yuan and Ng, 2012).

6.3.5. Sensitivity test for convergence criteria

Three simulations that are similarly treated, except for the convergence criterion, are conducted to test iterative convergence independence. In these three simulations, the scaled residuals for continuity, U-x, U-y, U-z, as well as energy κ and ω are given in Table 3. Similar with the statistical analysis performed for grid independence, this case study also conducts inferential statistics by using t-distribution to test the difference among the three wind data sets. The analysis results are tabulated in Tables 4a and 4b.

The p-value (<0.05) in the hypothesis test for criteria 1 and 3 (Table 4a) indicates a significant difference between two simulation results at the level of significance 0.05. But the p-value (>0.05) as shown in Table 4b indicates no significant difference between two simulation results in criteria 1 and 2 at the level of significance 0.05. These results indicate that the simulation results are independent of criteria 1 and 2.

To further clarify how different convergence criteria affect simulation accuracy, a scatter diagram is drawn as shown in Fig. 7. The larger variance in the low wind speed area (<1 m/s) indicates that the

Table 4a
Paired samples hypothesis test (the significant level: 0.05, sample size $n = 35$).

	Paired differences					t	Sig. (2-tailed) (P-value)
	Mean	Std. deviation	Std. error mean	95% Confidence interval of the difference			
				Lower	Upper		
Criterion_1–Criterion_3	−.05371	.11448	.01935	−.09304	−.01439	−2.776	.009

Table 4b
Paired samples hypothesis test (the significant level: 0.05, sample size $n = 35$).

	Paired differences					t	Sig. (2-tailed) (P-value)
	Mean	Std. deviation	Std. error mean	95% Confidence interval of the difference			
				Lower	Upper		
Criterion_1–Criterion_2	−.00001	.00005	.00001	−0.00003	.00001	−1.000	.324

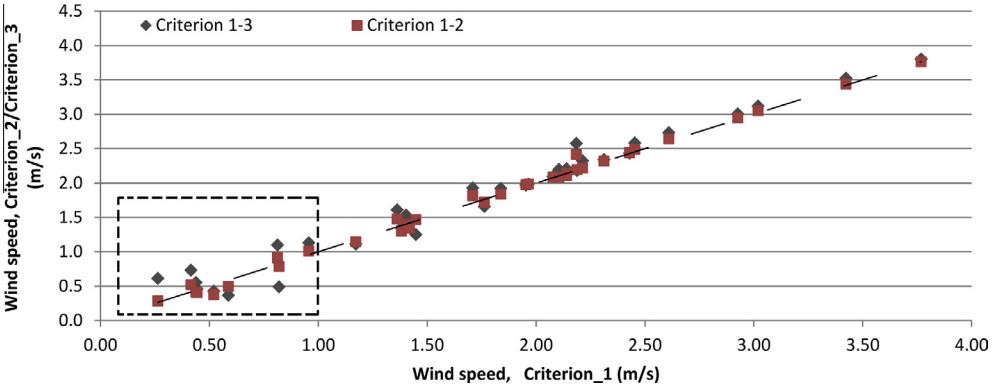

Fig. 7. Comparing results among three groups of wind data from the simulations with different iterative convergence criteria. Larger variance in the low wind speed area indicates that the simulation with the convergence criterion 3 is not sufficient in this case study.

simulation with the convergence criterion 3 fails to reproduce low-speed airflow. The evaluation on low-speed airflow is significantly important in this case study. Therefore, the scaled residuals in all of the scenarios have to be equal to or smaller than the ones in criterion 2 to ensure the accuracy of results, especially for low-speed airflow.

6.4. Simulation result analysis

In this section, by following the methods outlined in Section 5, the wind data are collected and analyzed to clarify the effects of different building design options on the surrounding pedestrian-level wind environment.

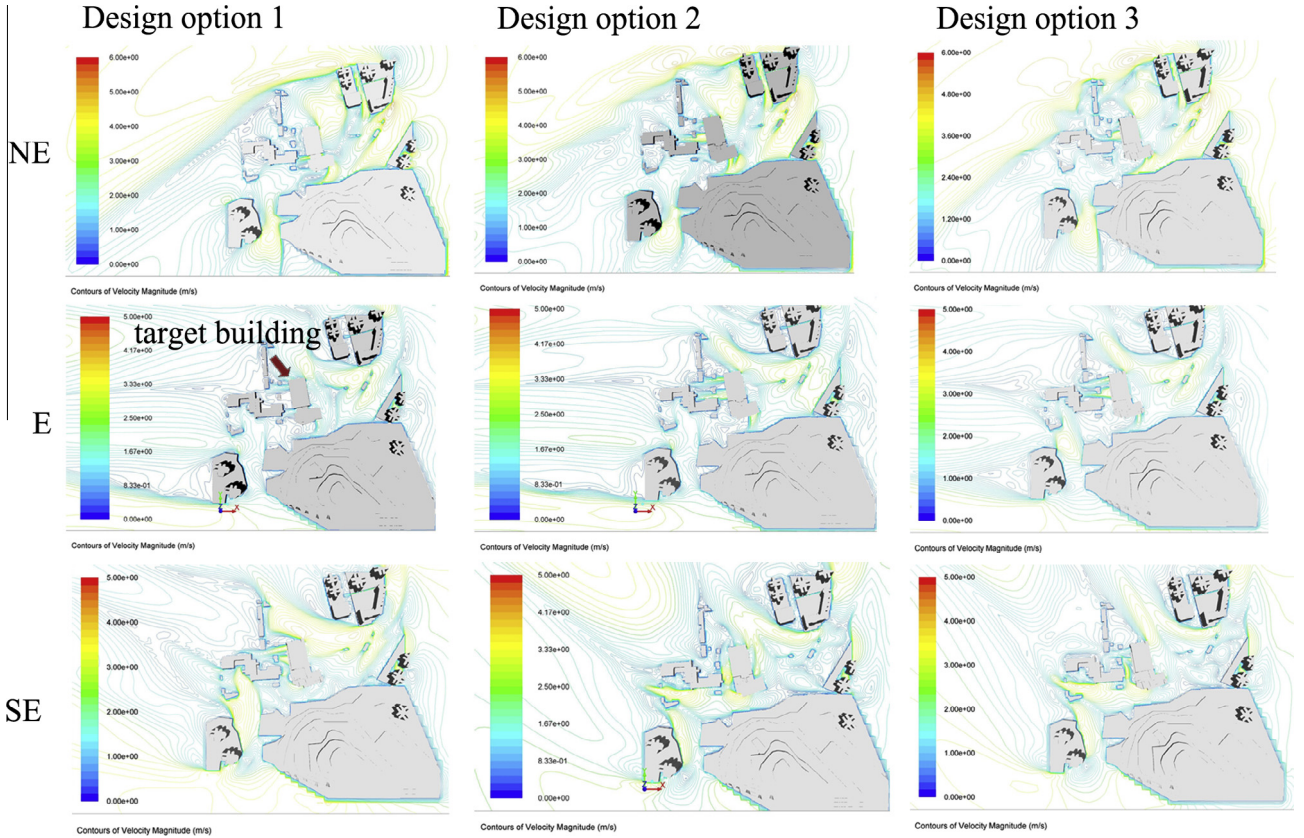

Fig. 8. Wind velocity contours in three design options and input wind directions.

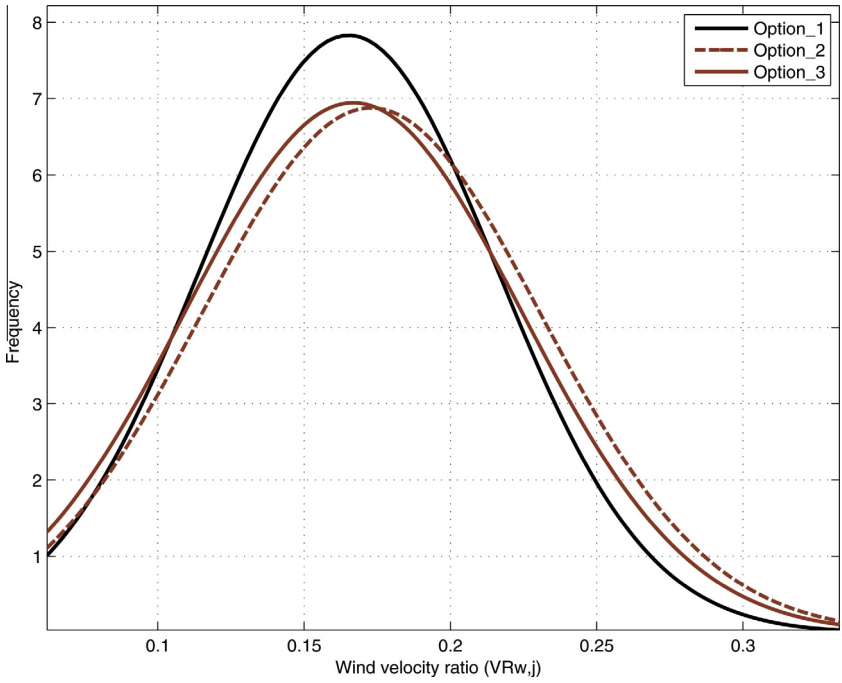

Fig. 9. Normal distribution fitting of $VR_{w,j}$ in design option 1, 2 and 3 (Confidence level $\alpha = 95\%$).

6.4.1. Global analysis

The wind velocity contour maps of 21 scenarios (three design options and seven wind directions), partly shown in Fig. 8, indicate that all design strategies in three design options are beneficial for the pedestrian-level wind environment surrounding the proposed building. Air can flow through the building porosities from the windward to the leeward areas. Option 1 is not as efficient as options 2 and 3, especially for the outdoor space of the secondary school and adjacent street (Fig. 8). It illustrates that the air passageways at the upper floor in design option 1 are not as efficient as that at the ground floor in design options 2 and 3 in terms of benefitting the pedestrian-level wind environment.

To verify the abovementioned understandings further, total 35 test points are selected at the pedestrian level for the statistical analysis, as shown in Fig. 6. Overall, the test points are evenly distributed and positioned in the surrounding open spaces, on the roads, and at places that pedestrians frequently access. The special test points are positioned in areas with strategic importance, such as test points 31 to 35 at the outdoor space of a secondary school (Fig. 6).

Overall wind velocity ratio ($VR_{w,j}$) at the test points is calculated, and the normal distribution fittings of $VR_{w,j}$ for all three design options are presented in Fig. 9. The pedestrian-level wind environments in two design options (options 2 and 3) are similar and strategies are evidently more efficient than that in design option 1.

6.4.2. Local analysis

Notably, the above averaged global evaluation could dilute the directional effects of the strategies and their advantages at the areas of strategic importance. Therefore, another cross-comparison, point by point, is conducted for the local analysis to further clarify the relationship between the design options and natural ventilation performance as well as to further cross-compare options 2 and 3.

The wind velocity ratio polar of the test points at the location with strategic importance (test points 1 and 31) are plotted in Tables 5 and 6. The wind polar is designed for seven inlet wind directions, and

Table 5
Test points 1 and 31. Special for 7 inlet wind directions and the length on the each direction means the respective value of VR.

Position	Wind velocity ratio polar (total 75.1% annual wind availability)
Test point _1	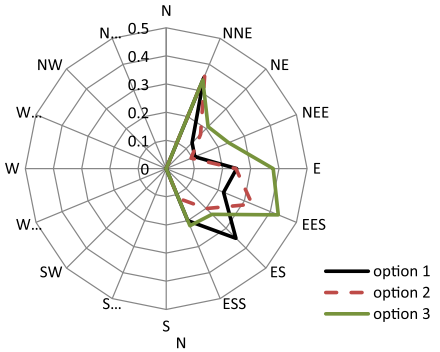
Test point _31	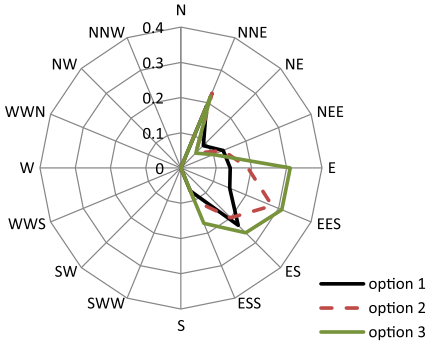

Table 6
Wind velocity rose at test point 24. Special for 7 inlet wind directions and the length on the each direction means the respective value of $V_{p,i,j}$.

Test point _24 $V_{p,i,24}$	
	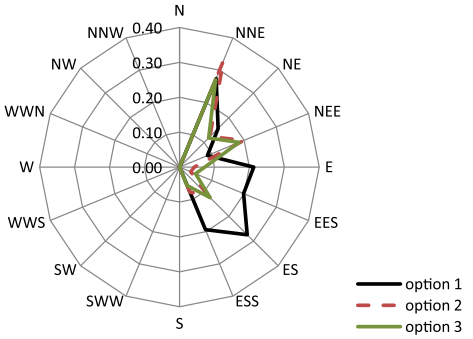

the lengths on the each direction represent the value of $VR_{i,j}$ in the different design options. Several important facts from the local analysis are as follows:

a) As shown in Table 5, the wind polar at test point 1 represents the wind environment at the adjacent street in different wind directions. The wind velocity ratio in design option 3 in the input wind directions NE, NEE, E, and EES is significantly higher than that in design options 1 and 2. This result cannot be reflected by the averaged global analysis, in which the performance of options 2 and 3 are similar.

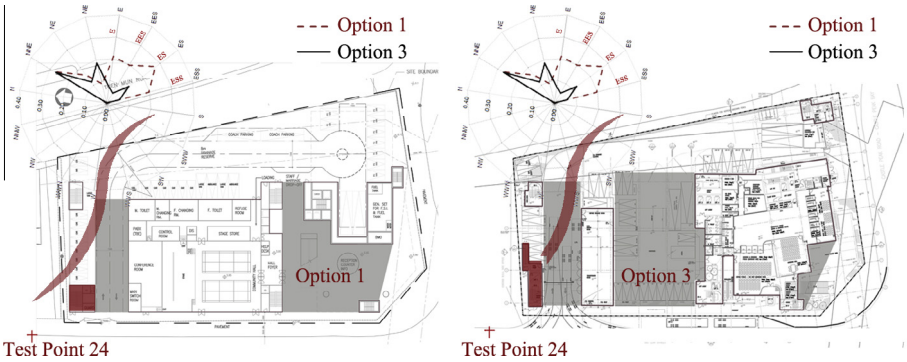

Fig. 10. Wind velocity ratios polar at the test point 24.The ground floor plan are presented together to illustrate how identify the part of the proposed building in option 3 that could block the incoming airflow.

b) As shown in Table 5, the wind polar at test point 31 compares the efficiency of the different design option strategies in terms of natural ventilation performance at the outdoor space in the secondary school. The wind velocity ratios in the input wind directions E, EES, ES, and ESS indicate that, among the three design options, the air can flow earliest through the proposed building in design option 3. Based on the above global and local analyses, the performances of options 2 and 3 are found to be globally better than that of option 1. At the location with strategic importance, design option 3 outperforms option 2.
c) Even after identifying the optimal design option, a more detailed understanding can be obtained to improve the optimal design option further. The wind velocity ratio polar in Table 6 indicates that the natural ventilation performance at test point 24 in design option 3 can be significantly poorer than that in design option 1. As shown in Fig. 10, combining the wind polar and ground floor planning, the limitation can be identified to the part of the building in option 3 that is highlighted by in red. An appropriate modification based on this understanding can significantly improve the annual averaged natural ventilation performance at the area close to test point 24.

6.5. Knowledge-based decision making

Based on the foregoing modeling and sufficient statistical analysis, the effects of different design options on the surrounding wind environment were well evaluated and cross-compared. Practical and accurate insights about optional design option identification and improvement are provided for architects. All mitigation strategies in design options 1, 2, and 3 are found to be helpful in mitigating the negative effects of the proposed building on the surrounding wind environment. However, the mitigation measurement in option 1 is not as sufficient as that in options 2 and 3. By adopting the measurements in option 2 or 3, natural ventilation performance can be significantly improved at the surrounding areas, especially at the adjacent street and the secondary school. Furthermore, based on the wind polar analysis, the performance of option 3 is found to be better than that of option 2 at several locations with strategic importance. Therefore, the design in option 3 is recommended as the optimal design option. Detailed modification recommendations for the design of option 3 are also provided based on wind velocity ratio polar analysis.

7. Conclusion

This study focuses on the practical application of CFD simulation to bridge the gap between wind engineering and architectural design. A procedural framework is provided by which to answer the questions encountered by wind consultants and architects, particularly those on input boundary condition setting, simulation modeling, verification, data collection and analysis for architectural design.

Finally, a Hong Kong case study is presented to illustrate that this framework and methods presented in this study can work well.

First, based on a broad literature review, this study clarifies how appropriate modeling methods can be selected to set the boundary condition for city/building scale modeling based on both particular modeling needs and available computer capability and input data sources.

Second, to ensure the accuracy CFD simulation in a real case study, apart from the setting requirements mentioned in the AIJ and COST 14 guidelines, this study provides the statistical methodology for the grid dependence and convergence criteria sensitivity test to validate modeling accuracy in practical applications. The application of the hypothesis testing (ANOVA) and regression analysis make the conclusions of the sensitivity tests robust and confident. For the practical CFD application, this statistical method is much more practical than validation method (cross-comparing with wind tunnel data) used in research works. The analysis result indicates that a reduction in the scaled residuals of at least three orders of magnitude could be acceptable in practical applications.

Finally, this study emphasizes the importance of data collection and analysis in the implementation of architectural design. The new data analysis process is presented from the global analysis based on referential statistics to the local analysis based on the wind velocity ratio polar. Due to this analysis process, reliable and detailed understandings of the relationship between the surrounding outdoor natural ventilation performances and building morphologies can be available to architects to easily identify critical design indexes and make the corresponding design decisions.

8. Limitation

In the high density cities, due to the very low wind speed in the street canyon, the buoyancy effects need to be considered and included into the CFD simulation technical guideline.

Acknowledgements

The study is supported by a Post Graduate Scholarship (PGS) grant from the Chinese University of Hong Kong and a contract research grant from Architecture Service Department of the Government of Hong Kong S.A.R. In particular, thanks are due to Professor Jimmy Fung of Hong Kong Science and Technology University for providing the MM5/CALMET data. The authors also wish to give special thanks to the referees for their valuable comments which help to improve the paper.

Appendix A

a. Symbols

d_{met}	Reference height (m)
H	Height of the tallest building on site (m)
n	Number of the test points
P	Annual probability of winds at a particular direction (%)
R_b	Blockage ratio
$U_{x,\ y,\ z}$	Wind speed in alongwind, crosswind, and vertical directions, respectively (m/s)
$V_{p,i,j}$	Wind velocity at the pedestrian level in a particular wind direction (i) at j-th test point (m/s)
$V_{i,}$	Wind velocity in a particular wind direction (i) at the reference height (d_{met}) (m/s)
V_h	Wind velocity in the input vertical wind profile (m/s)
$V_{met,\ i}$	Meteorology data of wind velocity at the reference height d_{met} in a particular wind direction (m/s)
V_{domain}	Volume of the computation domain (m^3)
V_{model}	Volume of the model (m^3)

$VR_{w,\,j}$	Overall wind velocity ratio at j-th test point
$VR_{i,j}$	Wind velocity ratio in the particular wind direction (i) at j-th test point
z_d	Zero-plane displacement height (m)
z_{min} and z_{max}	Layer boundary height for logarithmic wind profile (m)
z_0	Surface roughness length for momentum (m)
z_r	Blending height (m)
z_H	Averaged building height (m)
α	Surface roughness factor
δ	Boundary layer height (m)
κ_0	von Kármán constant
κ	Turbulent kinetic energy (m^2/s^2)
λ_f	Frontal area index
λ_p	Plan area fraction
ω	Specific turbulence dissipation rate (1/s)
b. Subscripts	
b	Blockage
i	Wind direction
j	Test point
x, y, z	Alongwind, crosswind, and vertical directions, respectively
met	Meteorology data
c.	*Abbreviations*
ku_d and ku_0	Kutzbach, J. Eqs. (15)
Le_0	Lettau, H. Eqs. (16)
Ra_0	Raupach, M. R., Eqs. (18)

References

Anderson, J.D., 2005. Ludwig Prandtl's boundary layer. Phys. Today 58, 42–48.

Architectural Institute of Japan (AIJ), 2007. AIJ guidebook for practical applications of CFD to pedestrian wind environment around buildings. Architectural Institute of Japan, ISBN: 978-4-8189-2665-3.

Arnfield, A.J., 2003. Two decades of urban climate research: a review of turbulence, exchanges of energy and water, and the urban heat island. Int. J. Climatol. 23, 1–26.

Ashie, Y., Hirano, K., Kono, T., 2009. Effects of Sea Breeze on Thermal Environment as a Measure against Tokyo's Urban Heat Island. The Seventh International Conference on Urban Climate, Yokohama, Japan.

Berg, L.K., Zhong, S.Y., 2005. Sensitivity of MM5-simulated boundary layer characteristics to turbulence parameterizations. J. Appl. Meteorol. 44, 1467.

Blocken, B., Stathopoulos, T., Carmeliet, J., 2007. CFD simulation of the atmospheric boundary layer: wall function problems. Atmos. Environ. 41, 238–252.

Blocken, B., Janssen, W.D., van Hooff, T., 2012. CFD simulation for pedestrian wind comfort and wind safety in urban areas: general decision framework and case study for the Eindhoven University campus. Environ. Modell. Softw. 30, 15–34.

Bottema, M., 1995. Parametization of aerodynamic roughness parameters in relation with air pollutant removal efficiency of streets. Air Pollution III. Computational Mechanics Publication 2, 235–242.

Bottema, M., 1996. Roughness parameters over regular rough surfaces: experimental requirements and model validation. J. Wind Eng. Ind. Aerodyn. 64, 249–265.

Chen, F., Kusaka, H., Bornstein, R., Ching, J., Grimmond, C.S.B., Grossman-Clarke, S., et al, 2011. The integrated WRF/urban modelling system: development, evaluation, and applications to urban environmental problems. Int. J. Climatol. 31, 273–288.

Cheng, V., Ng, E., Chan, C., Givoni, B., 2012. Outdoor thermal comfort study in a subtropical climate: a longitudinal study based in Hong Kong. Int. J. Biometeorol. 56, 43–56.

Counihan, J., 1971. Wind tunnel determination of roughness length as a function of fetch and roughness density of 3-dimensional roughness elements. Atmos. Environ. 5, 273–292.

Davenport, A.G., Grimmond, C.S.B., Oke, T.R., Wieringa, J., 2000. Estimating the roughness of cities and sheltered country. In: Proceedings of the 12th Conference on Applied Climatology, American Meteorological Society, Boston, 96–99.

Dudhia, J., 1993. A nonhydrostatic version of the Penn state-NCAR mesoscale model: validation tests and simulation of an Atlantic cyclone and cold front. Mon. Weather Rev. 121, 1493–1513.

European Environment Agency, 2006. Urban sprawl in Europe: the ignored challenge. European Environment Agency, Copenhagen.

Fluent Inc. FLUENT 14.0 theory Guide, 2012.

Frank, J., 2006. Recommendations of the COST action C14 on the use of CFD in predicting pedestrian wind environment. J. Wind Eng. 108, 529–532.

Frank, J., Sturm, M., Kalmbach, C., 2012. Validation of OpenFOAM 1.6.x with the German VDI guideline for obstacle resolving micro-scale models. Brussels, Belgium: COST, Office.
Garratt, J.R., 1978. Transfer characteristics for a heterogeneous surface of large aerodynamic roughness. Q. J. R. Meteorol. Soc. 104, 491–502.
Garreau, J., 1992. Edge City: Life on the New Frontier. Anchor Books, New York.
Gousseau, P., Blocken, B., Stathopoulos, T., Van HeijstG, J.F., 2010. CFD simulation of near-field pollutant dispersion on a high-resolution grid: a case study by LES and RANS for a building group in downtown Montreal. Atmos. Environ. 45, 428–438.
Grell, G.A., Dudhia, J., Stauffer, D.R., 1994. A description of the fifth-generation Penn State/NCAR Mesoscale Model (MM5). NCAR Technical Note NCAR/TN-398+STR. National Center for Atmospheric Research, Boulder, Colorado.
Grimmond, C.S.B., Oke, T.R., 1999. Aerodynamic properties of urban areas derived from analysis of surface form. J. Appl. Meteorol. 38, 1262–1292.
Hong Kong Building Department (HKBD), 2006. Sustainable building design guidelines. Practical note for authorized persons, registered structure engineers and registered geotechnical engineers. Hong Kong: APP-152.
Hong Kong Planning Department (HKPD), 2005. Feasibility study for establishment of air ventilation assessment system, Final report. The government of the Hong Kong Special Administrative Region.
Hong Kong Planning Department (HKPD), 2008. Urban climatic map and standards for wind environment – feasibility study, Working Paper 2B: Wind Tunnel Benchmarking Studies. Batch I, The Government of the Hong Kong Special Administrative Region.
Kubota, T., Miura, M., Tominaga, Y., Mochida, A., 2008. Wind tunnel tests on the relationship between building density and pedestrian-level wind velocity: development of guidelines for realizing acceptable wind environment in residential neighborhoods. Build. Environ. 43, 1699–1708.
Kutzbach, J., 1961. Investigations of the modifications of wind profiles by artificially controlled surface roughness. Section 7 of Studies of the three Dimentional Structure of the Planetary Boundary Layer. Annual Report. University of Wisconsin, pp. 71–113.
Lettau, H., 1969. Note on aerodynamic roughness-parameter estimation on the basis of roughness-element description. J. Appl. Meteorol. 8, 828–832.
Letzel, M.O., Krane, M., Raasch, S., 2008. High resolution urban large-eddy simulation studies from street canyon to neighbourhood scale. Atmos. Environ. 42, 8770–8784.
MacDonald, R.W., Griffiths, R.F., Hall, D.J., 1998. An improved method for the estimation of surface roughness of obstacle arrays. Atmos. Environ. 32, 1857–1864.
Mellor, G.L., Yamada, T., 1974. A hierarchy of turbulence closure models for planetary boundary layers. J. Appl. Meteorol. 13, 1791–1806.
Mellor, G.L., Yamada, T., 1982. Development of a turbulence closure model for geophysical fluid problems. Rev. Geophys. Space Phys. 20, 851–875.
Menter, F.R., Kuntz, M., Langtry, R., 2003. Ten years of industrial experience with the SST turbulence model. Turbulence, Heat Mass Transfer 4, 625–632.
Mochida, A., Murakami, S., Ojima, T., Kim, S., Ooka, R., Sugiyama, H., 1997. CFD analysis of mesoscale climate in the Greater Tokyo area. J. Wind Eng. Ind. Aerodyn. 67–68, 459–477.
Mochida, A., Tominaga, Y., Murakam, S., Yoshie, R., Ishihara, T., Ooka, R., 2002. Comparison of various κ-ε models and DSM applied to flow around a high-rise building – Report on AIJ cooperative project for CFD prediction of wind environment. Wind Struct. 5, 227–244.
Murakami, S., 2004. Indoor/outdoor climate design by CFD based on the software platform. Int. J. Heat Fluid Flow 25, 849–863.
Murakami, S., 2006. Environmental design of outdoor climate based on CFD. Fluid Dyn. Res. 38, 108–126.
Ng, E., 2009. Policies and technical guidelines for urban planning of high density cities – air ventilation assessment (AVA) of Hong Kong. Build. Environ. 44.
Ng, E., 2012. Towards a planning and practical understanding for the need of meteorological and climatic information for the design of high density cities – a case based study of Hong Kong. Int. J. Climatol. 32, 582–598.
Oke, T.R., 1987. Boundary layer climates, 2nd ed. Methuen, Inc., USA.
Oke, T.R., 2004. Sitting and exposure of meteorological instruments at urban sites. 27th NATO/CCMS International Technical Meeting on Air Pollution Modelling and Its Application, Banff.
Oke, T.R., 2006. Initial guidance to obtain representative meteorological observations at urban sites. World Meteorological Organization, 21–22.
Perry, S.G., Heist, D.K., Thompson, R.S., Snyder, W.H., Lawson, R.E., 2004. Wind tunnel simulation of flow and pollutant dispersal around the World Trade Centre site. Environ. Manager, 31–34.
Pielke, R.A., Cotton, W.R., Walko, C.J., Tremback, W.A.L., Grasso, L.D., Nicholls, M.D., et al, 1992. Comprehensive meteorological modeling system RAMS. Meteorol. Atmos. 49, 69–91.
Plate, E.J., 1982. Engineering Meteorology – Fundamentals of meteorology and their application to problems in environmental and civil engineering. Elsevier.
Plate, E.J., 1999. Methods of investigating urban wind fields—physical models. Atmos. Environ. 33, 3981–3989.
Raupach, M.R., 1992. Drag and drag partition on rough surfaces. Boundary Layer Meteorol. 60, 375–395.
Salim, S.M., Buccolieri, R., Chan, A., Di Sabatino, S., 2011. Numerical simulation of atmospheric pollutant dispersion in an urban street canyon: comparison between RANS and LES. J. Wind Eng. Ind. Aerodyn. 99, 103–113.
Scire, J.S., Robe, F.R., Fernau, M.E., Yamartino, R.J., 2000. A User's guide for the CALMET meteorological model (Version 5). Earth Tech, Concord, MA, USA.
Skamarock, W.C., Klemp, J.B., Dudhia, J., Gill, D.O., Barker, D.M., Wang, W., et al, 2005. A description of the advanced research WRF version 2. NCAR Technical Note. National Center for Atmospheric Research.
Tominaga, Y., Mochida, A., Yoshie, R., Kataoka, H., Nozu, T., Yoshikawa, M., et al, 2008. AIJ guidelines for practical applications of CFD to pedestrian wind environment around buildings. J. Wind Eng. Ind. Aerodyn. 96, 1749–1761.
Yamada, M., Bunker, S., 1989. Development of a nested grid, second moment turbulence closure model and data simulation. J. Appl. Meteorol. 27, 562–578.

Yim, S.H.L., Fung, J.C.H., Lau, A.K.H., Kot, S.C., 2007. Developing a high-resolution wind map for a complex terrain with a coupled MM5/CALMET system. J. Geophys. Res. 112. http://dx.doi.org/10.1029/2006JD007752.
Yoshie, R., Mochida, A., Tominaga, Y., Kataoka, H., Harimoto, K., Nozu, T., et al, 2007. Cooperative project for CFD prediction of pedestrian wind environment in the Architectural Institute of Japan. J. Wind Eng. Ind. Aerodyn. 95, 1551–1578.
Yuan, C., Ng, E., 2012. Building porosity for better urban ventilation in high-density cities – a computational parametric study. Build. Environ. 50, 176–189.